https://doi.org/10.5194/egusphere-2026-3167
Preprint. Discussion started: 19 June 2026

Quantifying canopy CO_2 storage to improve long-term estimates of net ecosystem carbon exchange in the southern Amazon forest

Bárbara Antonucci[1], Raoni A. Santana[2,1], Nara L. R. Andrade[3], Eliane Gomes Alves[4,1], Santiago Botía[5], Carla M.A. Souza[5], Anne C. S. Mendonça[1], Shujiro Komiya[4], Denisi H. Hall[1], Natalia Restrepo-Coupe[6], Gabriel B. Costa[2], and Cléo Q. Dias-Júnior[1]

[1]Postgraduate Program in Climate and Environment, National Institute of Amazonian Research (INPA), Manaus, AM, Brazil
[2]Institute of Engineering and Geosciences, Federal University of Western Pará (UFOPA), Santarém, PA, Brazil
[3]Department of Sanitary and Environmental Engineering, Federal University of Rondônia Foundation (UNIR), Ji-Paraná, Rondônia, Brazil
[4]Department of Biogeochemical Processes, Max Planck Institute for Biogeochemistry (MPI-BGC), Jena, Germany
[5]Biogeochemical Signals, Max Planck Institute for Biogeochemistry (MPI-BGC), Jena, Germany
[6]Department of Ecology and Evolutionary Biology, The University of Arizona (UA), Tucson, Arizona, USA

Correspondence: Bárbara Antonucci (antonucciengenharia@gmail.com)

Abstract.

The Amazon rainforest plays a critical role in the global carbon cycle, yet large uncertainties remain regarding its net carbon balance. Accurate estimates of net ecosystem exchange (NEE) require accounting for the CO_2 storage term, which is commonly derived from vertical CO_2 profile measurements that are scarcely available at long-term flux tower sites. Here, we evaluated three approaches for estimating canopy CO_2 storage at the Rebio Jaru forest site in Rondônia, Brazil: (1) a multi-point CO_2 profile (MPP), (2) a single-point profile (SPP) based on a closed-path gas analyzer, and (3) a single-point eddy covariance approach (SPE) using CO_2 measurements from an open-path gas analyzer. Although the methods operated simultaneously for less than two years, both simplified approaches showed strong agreement with the reference MPP method, with coefficients of determination of $R^2 = 0.87$ for SPP and $R^2 = 0.79$ for SPE, whereas neglecting the storage term resulted in poor agreement ($R^2 = 0.24$). Using the SPE approach, we reconstructed a 13-year NEE time series that revealed pronounced interannual variability, with the forest generally acting as a carbon sink during La Niña conditions and shifting toward a carbon source during El Niño events and during consecutive years due to drought legacy effects. The seasonal cycle exhibited a marked carbon source peak during the transition from the dry to the wet season, likely associated with enhanced litter decomposition and increased soil respiration following the first rainfall events after prolonged dry periods. These results demonstrate that simplified single-point approaches can reliably reconstruct long-term NEE dynamics and substantially improve estimates of Amazonian carbon balance at sites where complete CO_2 profile measurements are unavailable.

Keywords. Amazon rainforest, net ecosystem exchange, CO_2 storage flux, eddy covariance, ENSO

https://doi.org/10.5194/egusphere-2026-3167
Preprint. Discussion started: 19 June 2026

1 Introduction

The Amazon rainforest plays a crucial role in the global carbon cycle and is widely recognized as a key component in regulating Earth's climate. However, the combined effects of deforestation, recurrent droughts (Doughty et al., 2015; Marengo et al., 2024), and rising temperatures provide increasing evidence of a transition from a carbon sink to a carbon source (Davidson et al., 2012; Tavares et al., 2023; Flores et al., 2024; Botía et al., 2026). This transition appears particularly pronounced in southeastern Amazonia, where a net CO_2 source has already been observed (Gatti et al., 2021). In this context, Gatti et al. (2021) showed that the Amazon has become a net carbon source of 0.29 PgC yr^{-1}, driven by historical degradation in the southeastern portion of the region. Nevertheless, Botía et al. (2025) revised these estimates by applying humidity corrections to atmospheric measurements, identifying a near-neutral balance (-0.04 PgC yr^{-1}), although the regional balance remains affected by emissions from the adjacent Cerrado and Caatinga biomes. More recently, Botía et al. (2026) demonstrated that this neutrality is highly sensitive to climatic anomalies; during the 2023 El Niño event, the basin rapidly shifted to a temporary carbon source, with emissions ranging between 0.15 and 0.20 PgC, affecting even preserved areas.

A representative example of this environmental shift is the Jaru Biological Reserve (Rebio Jaru), located within the "Arc of Deforestation" (Csillik et al., 2024). This region contains large areas of fragmented and degraded forests, characterized by increasing edge effects and the progressive loss of original forest structure (Feitosa et al., 2023; Trejo et al., 2025). Subjected to intense anthropogenic pressure and highly vulnerable to drought, Rebio Jaru reflects broader processes occurring across the southern Amazon and is therefore an important site for understanding regional forest carbon balance dynamics (Chen et al., 2024).

Proper monitoring of CO_2 fluxes between the biosphere and the atmosphere is essential for determining whether a region acts as a carbon source or sink. Robust quantification of net ecosystem exchange (NEE) is one of the most effective direct approaches for assessing ecosystem carbon balance over time (Baldocchi et al., 2024). However, accurate NEE estimation requires accounting for the storage term (F_s), which represents the CO_2 accumulated in the air column beneath the flux-measurement sensors (Aubinet et al., 2012). This component becomes particularly important during periods of low atmospheric turbulence (Acevedo et al., 2009; Peltola et al., 2021). Ideally, F_s should be calculated using detailed vertical CO_2 concentration profiles measured at multiple heights, typically at least six levels, to capture the complex stratification within the canopy air space (Aubinet et al., 2012). Such multi-level instrumentation is essential for robust NEE estimates in dense vegetation, including tropical and temperate forests (Buchmann et al., 1997; Hutyra et al., 2008; Araújo et al., 2010; Paul-Limoges et al., 2017; Rodrigues et al., 2024).

Despite its importance, maintaining complete vertical CO_2 concentration profiles over long periods is often difficult at remote Amazonian sites because of major logistical constraints. These include complex maintenance requirements, frequent power supply interruptions, and rapid degradation of sensors and cables caused by high humidity and biological activity. Consequently, there is a clear need to evaluate simpler yet reliable methods for estimating the storage term that can be applied to long-term flux datasets.

https://doi.org/10.5194/egusphere-2026-3167
Preprint. Discussion started: 19 June 2026

Several approaches have been proposed to estimate F_s when measurements at multiple heights are unavailable. One widely used method, introduced by Hollinger et al. (1994), assumes that temporal variations in CO_2 concentration measured at a single reference height (typically from the eddy covariance gas analyzer) represent the entire air column below the sensor. Early evaluations of this approach reported relatively small errors in daily carbon balance estimates. For example, Greco and Baldocchi (1996) found that the residual error associated with this approximation averaged approximately -0.20 ± 2.32 gC m^{-2} day^{-1} over 24-hour periods, suggesting that uncertainties introduced by omitting the full vertical profile are relatively small compared with those associated with gradient systems.

Another approach involves reconstructing the vertical distribution of CO_2 by assuming a theoretical profile, such as a logarithmic function of the form $C(z) = a + b\ln(z)$, consistent with canopy micrometeorological theory (Finnigan, 2004; Aubinet et al., 2012). This allows estimation of F_s even with measurements at a limited number of heights. More recently, data-driven approaches have also been proposed to reconstruct storage fluxes when observational data are incomplete. Machine learning techniques can be used to predict F_s based on meteorological and eddy covariance variables, including CO_2 concentration measured by the eddy covariance system, air temperature, vapor pressure deficit (VPD), friction velocity (u^*), wind speed, and incoming radiation. In this approach, F_s values calculated from periods with available profile measurements are used to train regression models, which are then applied to reconstruct the storage flux during periods without vertical profile observations (Pastorello et al., 2020).

Previous studies in the Amazon have addressed the lack of multi-level CO_2 profiles by simplifying the storage term to single-point measurements or by restricting analyses to periods of strong atmospheric turbulence (von Randow et al., 2004; Cirino et al., 2014). Other studies incorporated advection components to better represent complex flow dynamics, as performed at the Cuieiras Reserve (Araújo et al., 2002) and the Tapajós National Forest (Tóta et al., 2008).

In this study, we evaluate the single-point storage estimation approach proposed by Hollinger et al. (1994), which uses CO_2 concentration measurements from a single height to estimate F_s. Previous studies comparing single-point and multi-point approaches indicate that the performance of this method depends strongly on atmospheric turbulence conditions. For example, Saito et al. (2005) reported that the single-point approach underestimated the storage term by approximately 22% under low-turbulence conditions, whereas Moureaux et al. (2008) found only a 6% overestimation under well-mixed conditions. Together, these studies suggest that simplified storage estimates can provide reliable results when atmospheric mixing is sufficiently strong.

Here, we present the first long-term (13-year) evaluation of single-point CO_2 storage estimation at an Amazon forest site and investigate its implications for NEE variability under different climatic conditions. Using long-term flux measurements collected at Rebio Jaru, we assess the performance of this approach and reconstruct the NEE time series for one of the oldest flux tower sites in Amazonia, where complete vertical CO_2 profile measurements were available only for a limited period. This reconstruction allows us to evaluate whether this portion of the southern Amazon currently behaves as a net carbon sink or source. In addition, the approach tested here can be extended to other Amazonian sites, providing a practical framework for investigating regional carbon dynamics using long-term flux observations.

https://doi.org/10.5194/egusphere-2026-3167
Preprint. Discussion started: 19 June 2026

Table 1. Overview of measured variables, micrometeorological sensors, gas instrumentation, and measurement heights at the tower.

Variable	Description	Instrument	Sampling rate (Hz)	Heights (m)
u, v, w, T_s	Turbulent 3D wind speed and sonic temperature	Sonic anemometer	10	63.4
c, q	CO_2 and H_2O concentration	Infrared gas analyzer	10	63.4
c	CO_2 concentration	Closed-path infrared gas analyzer	0.0167	2, 12, 22, 34, 50, 62
T_{air}	Air temperature	Thermohygrometer	0.00056	62
S_{in}	Shortwave solar radiation	Pyranometer	0.00056	52
P	Precipitation	Rain gauge	0.00056	62

2 Material and Methods

2.1 Site Description and Measurements

The Rebio Jaru is a fully protected conservation unit covering approximately 350,000 hectares in the state of Rondônia, Brazil. The vegetation is predominantly classified as Open Ombrophilous Forest (Culf et al., 1997) and is also characterized as semideciduous or seasonally dry forest (Costa et al., 2010). The leaf area index (LAI) exhibits a marked seasonal cycle, varying from 5.56 [5.44–5.69] $m^2\,m^{-2}$ in July to 6.53 [6.26–6.74] $m^2\,m^{-2}$ in January (Barbino et al., 2023). A 62 m tall micrometeorological tower (10.19° S, 61.87° W), part of the Large-Scale Biosphere–Atmosphere Program (LBA), has been operational at the site since 1999 (Fig. 1). The regional climate is characterized by a mean annual precipitation of approximately 2200 mm (Gomes et al., 2015; Antonucci et al., 2025). The site elevation is approximately 220 m above sea level, and the vegetation has an average canopy height of 33 m, with emergent trees reaching nearly 45 m (Rummel et al., 2002).

Measurements at the site have been conducted continuously since early 1999, making this one of the longest-running micrometeorological monitoring towers currently operating in the Amazon. In 2003, a temporary interruption occurred due to the relocation of the tower; however, the continuity of the CO_2 measurement series was maintained, as reported by Aguiar et al. (2012). Measurements resumed in 2004 at the current tower location. Additional data gaps occurred during subsequent periods, primarily associated with limitations in financial support and logistical constraints.

Fig. 2 presents the temporal evolution of the instrumentation deployed at the site between 1999 and 2020, including eddy covariance systems, CO_2 profile measurements, and supporting meteorological observations. The long-term observational program involved successive replacements of sonic anemometers and infrared gas analyzers while preserving the continuity and consistency of the atmospheric monitoring record. Eddy covariance flux measurements and CO_2 profile observations were simultaneously available only during a restricted period, from March 2008 to September 2009. Additional information regarding the measured variables, sensor models, sampling rate and measurement heights is provided in Table 1 and Fig. 2.

https://doi.org/10.5194/egusphere-2026-3167
Preprint. Discussion started: 19 June 2026

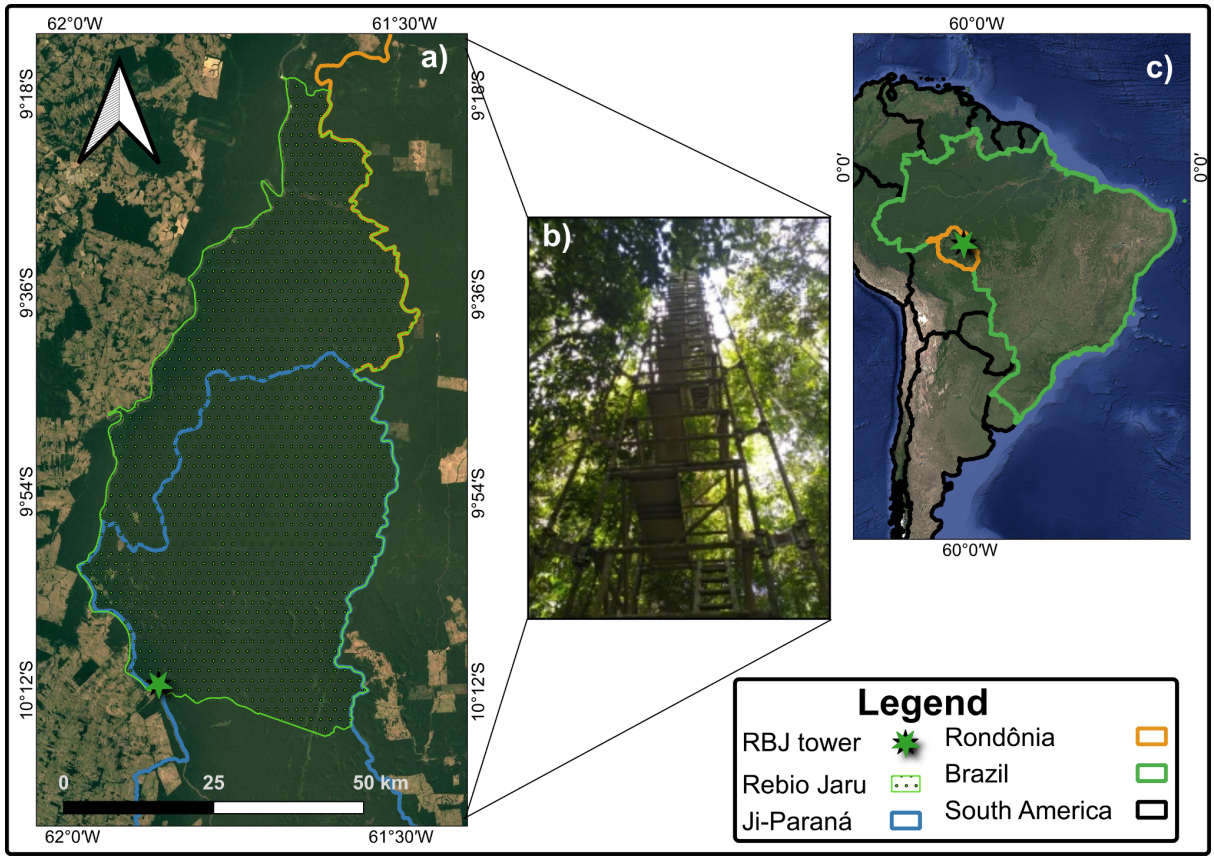

Figure 1. Location and infrastructure of the study site. (a) Spatial delimitation of the Jaru Biological Reserve (Rebio Jaru), Rondônia, Brazil; (b) view of the micrometeorological tower (LBA site); (c) geographic position of the study area in South America. The map was generated using satellite imagery from Google Earth (Google, 2026) and cartographic data from the Brazilian Institute of Geography and Statistics (IBGE, 2022).

2.2 Determination of the Net Ecosystem CO_2 Exchange

Assuming steady-state turbulent flow and horizontal surface homogeneity, net ecosystem exchange (NEE) was calculated as the sum of the turbulent CO_2 flux (F_c) and the storage flux (F_s) (Aubinet et al., 2012):

$$\mathrm{NEE} = F_c + F_s \tag{1}$$

The turbulent flux was obtained from high-frequency eddy covariance measurements as:

$$F_c = \overline{w'c'} \tag{2}$$

https://doi.org/10.5194/egusphere-2026-3167
Preprint. Discussion started: 19 June 2026

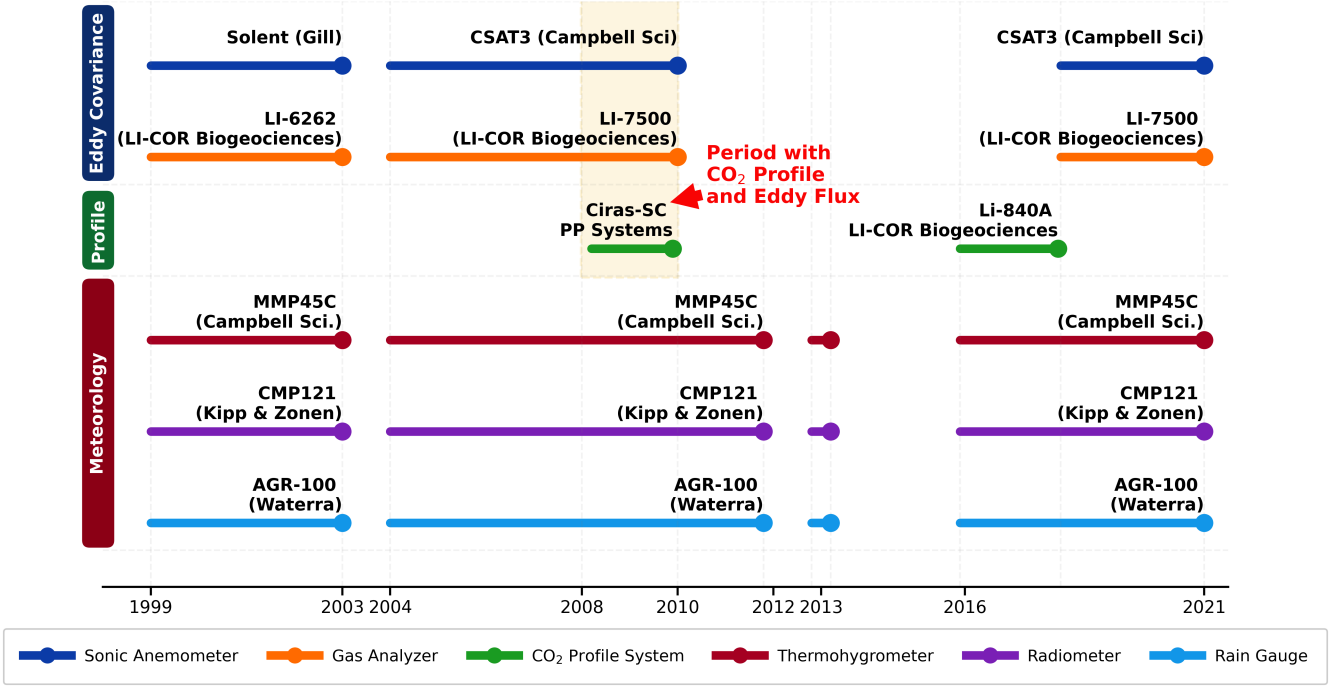

Figure 2. Models of instruments and their operational periods at the Rebio Jaru site from 1999 to 2021. The largest data gaps occurred in 2003 and between 2011 and 2015.

where w' is the fluctuation of the vertical wind velocity and c' is the fluctuation of the CO_2 concentration.

The storage flux represents the temporal change in CO_2 content within the air column between the surface and the integration height (z). Assuming constant dry air density (ρ), it can be expressed as (Baldocchi and Meyers, 1988; Aubinet et al., 2012):

$$F_s(t) = \rho \int_0^z \frac{\partial c(z,t)}{\partial t}\, dz \tag{3}$$

In this study, F_s was calculated using three approaches: (i) multi-point profile (MPP), (ii) single-point profile (SPP), and (iii) single-point eddy (SPE). These approaches were derived from Eq. (3).

The MPP method uses CO_2 concentrations measured at discrete heights and can only be calculated when the complete CO_2 profile is available ($z_1, z_2, \ldots, z_n$), requiring a numerical approximation of the vertical integral:

$$F_s(t_i) = \rho \sum_{i=1}^{n} \left(\frac{c_i(t+\Delta t) - c_i(t)}{\Delta t} \right) \Delta z_i \tag{4}$$

where c_i is the CO_2 concentration at height z_i, Δt is the time interval between measurements, and Δz_i is the vertical layer thickness associated with each level.

https://doi.org/10.5194/egusphere-2026-3167
Preprint. Discussion started: 19 June 2026

For the SPP and SPE approaches, the CO_2 concentration was assumed to be vertically uniform between the surface and the measurement height. Applying a finite-difference approximation to Eq. (3) yields:

$$F_s(t) \approx \rho\, z \frac{\partial c(t)}{\partial t} \approx \rho\, z \frac{c(t+\Delta t) - c(t)}{\Delta t} \tag{5}$$

Equation (5) was applied using the CO_2 concentration measured at 62 m for the SPP approach, whereas for the SPE approach the CO_2 concentration was obtained from the open-path infrared gas analyzer installed at 63.4 m.

Atmospheric turbulence intensity was characterized by the friction velocity (u^*):

$$u^* = \left[\left(\overline{u'w'}\right)^2 + \left(\overline{v'w'}\right)^2 \right]^{1/4} \tag{6}$$

where u' and v' are the fluctuations in the longitudinal and lateral wind components, respectively.

Atmospheric stability was evaluated using the dimensionless stability parameter z/L, defined according to Monin–Obukhov similarity theory as:

$$\frac{z}{L} = -\frac{\kappa g z \overline{w'\theta'_v}}{\overline{\theta_v}\, u^{*3}} \tag{7}$$

where κ is the von Kármán constant (0.4), g is the gravitational acceleration, $\overline{w'\theta'_v}$ is the kinematic virtual potential temperature flux, $\overline{\theta_v}$ is the mean virtual potential temperature, and u^* is the friction velocity. Atmospheric stability conditions were classified according to the value of z/L as: very unstable ($z/L < -3$), unstable ($-3 \le z/L < -0.1$), neutral ($-0.1 \le z/L \le 0.1$), stable ($0.1 < z/L < 2$), and very stable ($z/L \ge 2$).

2.3 Processing and quality control

Eddy covariance fluxes averaged over 30-minute intervals, including CO_2 exchange, were computed using the Alteddy software for the 1999–2010 period. For subsequent years, fluxes were processed using EddyPro (LI-COR, Lincoln, NE, USA). Both software packages were configured using standardized processing routines to ensure consistency and comparability throughout the long-term dataset.

The processing chain included double-axis coordinate rotation to align the coordinate system with the mean wind direction, forcing the mean vertical wind velocity component (w) to zero. Additional procedures included time-lag compensation, frequency response corrections, and corrections for cross-wind effects, humidity, and sonic temperature. The Webb–Pearman–Leuning (WPL) correction was applied to account for air-density fluctuations (Aubinet et al., 2012).

F_s and NEE were calculated separately using the outputs generated by Alteddy and EddyPro. An additional quality-control routine was implemented to remove physically inconsistent values and periods affected by instrumental malfunction, including NEE spikes exceeding $\pm 50\,\mathrm{mol\,m^{-2}\,s^{-1}}$. Data collected during rainfall events, when water droplets obstructed the sonic anemometer measurement path, were also excluded from the analysis.

https://doi.org/10.5194/egusphere-2026-3167
Preprint. Discussion started: 19 June 2026

To minimize the underestimation of nighttime respiration under stable atmospheric conditions, a u^* threshold was applied to filter periods with insufficient turbulence. The definition of an appropriate u^* threshold is widely recognized as one of the main sources of uncertainty in NEE estimates (Aubinet et al., 2012), particularly in Amazon forests, where strong decoupling often occurs between the air below and above the canopy (Santana et al., 2018). Miller et al. (2004) evaluated different u^* thresholds by comparing NEE derived from eddy covariance measurements with independent inventory-based estimates for a forest near Santarém, Pará, Brazil, and reported an optimal threshold of $0.2\,\mathrm{m\,s^{-1}}$, which excluded approximately 60% of the nocturnal data.

However, applying a threshold of $0.2\,\mathrm{m\,s^{-1}}$ to the Rebio Jaru site would remove more than 90% of the nighttime observations. Therefore, a site-specific threshold corresponding to the exclusion of 60% of the nocturnal data was adopted for Rebio Jaru, resulting in a u^* threshold of $0.12\,\mathrm{m\,s^{-1}}$. The same threshold was applied throughout the entire dataset, since the seasonal variability of u^* was relatively small, as shown in Fig. 3.

Finally, remaining gaps in the dataset were filled using a modified Marginal Distribution Sampling (MDS) approach based on temporal similarity (Reichstein et al., 2005). The algorithm reconstructed missing values using averages from observations acquired at the same half-hourly time step within moving temporal windows of ±7, ±14, and ±30 days, requiring a minimum number of valid samples for gap filling. Long gaps exceeding 90 days were not reconstructed.

3 Results and Discussion

3.1 Characterizing meteorology

The observational record from the Rebio Jaru tower is not sufficiently long to establish a local climatological normal, which conventionally requires at least 30 years of continuous measurements. Therefore, long-term precipitation data from the municipality of Porto Velho, Rondônia, Brazil, the nearest location with an extended meteorological record, were used as a regional climatological reference. Both precipitation time series are presented in Fig. 3.

Precipitation distribution is characterized by marked seasonality, with the wet season presenting average monthly totals above 250 mm at Rebio Jaru and the dry season showing precipitation below 100 mm between May and September. The Porto Velho climatology presents slightly higher precipitation values in some months, such as January, likely associated with geographical and land-cover differences between the two regions. Nevertheless, the seasonal pattern remains consistent, reinforcing the robustness and representativeness of the rainfall regime observed at Rebio Jaru (Antonucci et al., 2025).

Shortwave radiation exhibits its lowest values during the peak the rainy season, from December to March, when persistent cloud cover limits incoming solar radiation. As rainfall decreases and cloudiness is reduced, radiation progressively increases from April onward, reaching maximum values during the dry season, particularly in July and August (approximately $225\,\mathrm{W\,m^{-2}}$). During this period, clearer skies allow greater solar input to reach the surface, enhancing surface heating and atmospheric instability (Aguiar et al., 2012). From September onward, shortwave radiation gradually declines with the onset of the wet season and the associated increase in cloud formation and precipitation.

https://doi.org/10.5194/egusphere-2026-3167
Preprint. Discussion started: 19 June 2026

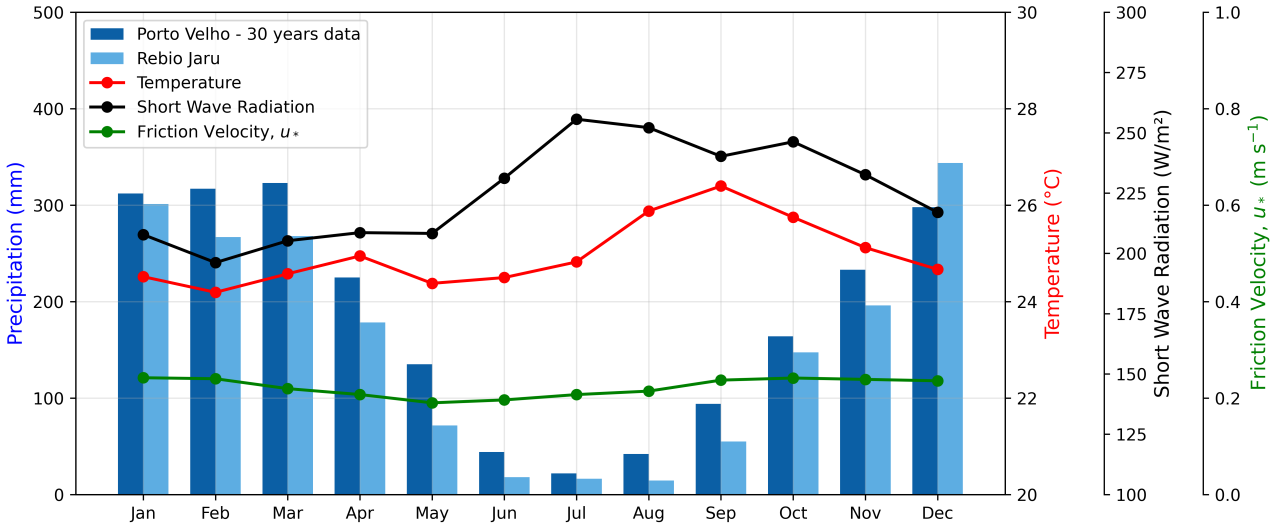

Figure 3. Monthly seasonal cycle of precipitation, air temperature, incoming shortwave radiation, and friction velocity (u_*). Light blue bars represent the monthly accumulated precipitation at Rebio Jaru (13 years of data), while dark blue bars represent the 30-year mean monthly precipitation from Porto Velho, Rondônia.

Between May and September, the region is frequently influenced by incursions of polar air masses (Garreaud, 1999; Fisch et al., 2004). These events, locally known as *friagens*, strongly affect Rebio Jaru and contribute to reductions in average air temperature to approximately 25 °C during the May–July period (Fig. 3). Such episodes typically last from two to four days and can produce sharp decreases in minimum temperature, reaching extremes of 13 °C in 2001 (de Oliveira et al., 2004) and 11 °C in 2017 (Antonucci et al., 2023).

3.2 Evaluation of the single-point CO_2 storage flux

The diurnal cycle of the F_s is strongly controlled by atmospheric stability regimes. During nighttime, ecosystem respiration combined with weak turbulence promotes CO_2 accumulation within and above the canopy, leading to progressively larger positive F_s values throughout the night, as shown in Fig. 4. Similar behavior was reported for the Tapajós National Forest in Pará, Brazil, by Hutyra et al. (2008).

After sunrise, increasing solar radiation enhances turbulent mixing and promotes flushing events that transport CO_2-rich air from the sub-canopy to the tower top, mainly during very calm nights. As a consequence, F_s increases rapidly, frequently exceeding 30 $\mu mol\, m^{-2}\, s^{-1}$, a pattern commonly observed in forest ecosystems (Araújo et al., 2002).

Following the morning transition, photosynthetic activity intensifies and the forest begins to act as a carbon sink. Consequently, F_s becomes negative, indicating net CO_2 uptake by the ecosystem. During this period, storage fluxes can reach magnitudes close to 40 $\mu mol\, m^{-2}\, s^{-1}$ Fig. 4).

https://doi.org/10.5194/egusphere-2026-3167
Preprint. Discussion started: 19 June 2026

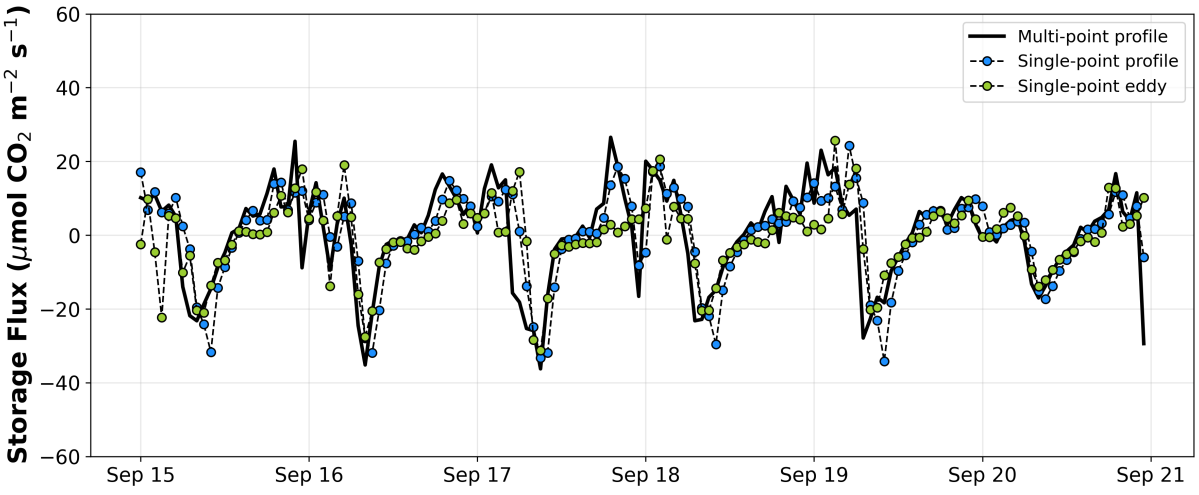

Figure 4. Example of the diurnal evolution of CO_2 storage flux (F_s) during 15–21 September 2008 at the Rebio Jaru site. Storage was calculated using the multi-point profile (MPP), single-point profile (SPP), and single-point eddy (SPE) methods.

The overall behavior shown in Fig. 4 is remarkably consistent among the three methods studied here, with all approaches capturing the same diurnal patterns, including the pronounced nocturnal accumulation and daytime depletion of CO_2. In other words, both single-point methods capture the main characteristics of the behavior exhibited by the multi-point profile (MPP) method, even though small differences occur in the instantaneous measurements between the methods.

The comparison between storage estimates using single-point profile (SPP) and single-point eddy (SPE) against MPP across stability regimes reveals a clear dependence on atmospheric stability, with generally stronger agreement under more turbulent conditions and a progressive decline in skill as stratification increases (Table 2). Both SPP and SPE show improved and more coherent relationships with MPP, particularly under very unstable, unstable, and neutral conditions, where enhanced turbulent mixing promotes stronger vertical coupling.

As atmospheric stability increases further, both methods show a clear degradation in performance, although the decline is more pronounced for SPE. In stable conditions, SPP remains relatively robust ($R^2 = 0.81$), outperforming SPE ($R^2 = 0.62$), with both methods showing comparable RMSE values and moderate biases. Under very stable conditions, performance deteriorates substantially, especially for SPE, which exhibits very low agreement with MPP ($R^2 = 0.09$) and a large bias (3.51), indicating a breakdown in its ability to capture storage variability. SPP also weakens ($R^2 = 0.37$) but retains some predictive skill and more stable error characteristics. Overall, SPP consistently shows lower RMSE and more stable behavior across regimes, while SPE is more sensitive to stability, particularly under strongly stratified conditions. These results confirm that storage estimates are most reliable under turbulent conditions and progressively deteriorate with increasing atmospheric stability.

In the very unstable regime, SPP achieves strong agreement with MPP ($R^2 = 0.85$), while SPE shows slightly lower skill ($R^2 = 0.71$) with larger RMSE values. Similarly, in unstable conditions, SPP remains robust ($R^2 = 0.83$) and exhibits the

https://doi.org/10.5194/egusphere-2026-3167
Preprint. Discussion started: 19 June 2026

Table 2. Statistical comparison between the multi-point profile storage method (MPP) and the two single-point approaches across atmospheric stability classes. The coefficient of determination (R^2), root mean square error (RMSE), and mean bias are shown for each comparison.

Stability class	Comparison	R^2	RMSE (μmol m^{-2} s^{-1})	Bias (μmol m^{-2} s^{-1})
Very Unstable	SPP vs. MPP	0.85	5.37	2.43
Very Unstable	SPE vs. MPP	0.71	7.63	1.59
Unstable	SPP vs. MPP	0.83	4.83	4.42
Unstable	SPE vs. MPP	0.68	6.30	-0.19
Neutral	SPP vs. MPP	0.74	5.57	1.95
Neutral	SPE vs. MPP	0.65	6.04	0.74
Stable	SPP vs. MPP	0.81	5.03	2.74
Stable	SPE vs. MPP	0.62	6.92	0.07
Very Stable	SPP vs. MPP	0.37	5.49	-0.33
Very Stable	SPE vs. MPP	0.09	6.71	3.51

SPP: single-point profile method; SPE: single-point eddy covariance method; MPP: multi-point profile method.

lowest RMSE (4.83), whereas SPE shows lower explanatory power ($R^2 = 0.68$) and higher RMSE (6.30), despite a relatively small bias (-0.19). In the neutral regime, performance decreases slightly for both methods, although SPP retains stronger skill ($R^2 = 0.74$) than SPE ($R^2 = 0.65$) and maintains lower RMSE values.

Fig. 5 shows the relationship between the NEE calculated using F_s from the MPP ($\mathrm{NEE_{MPP}}$) and the NEE calculated using alternative approaches for estimating F_s: (a) SPP ($\mathrm{NEE_{SPP}}$); (b) SPE ($\mathrm{NEE_{SPE}}$); and (c) $F_s = 0$ (i.e., NEE $= F_c$). The results reveal that the highest coefficient of determination ($R^2 = 0.87$) was observed between $\mathrm{NEE_{MPP}}$ and $\mathrm{NEE_{SPP}}$ (Fig. 5a).

Likewise, the comparison between $\mathrm{NEE_{MPP}}$ and $\mathrm{NEE_{SPE}}$ (Fig. 5b) also showed a strong correlation ($R^2 = 0.79$). These similarities indicate that the temporal variability of CO_2 storage in Rebio Jaru is largely controlled by concentration changes near the upper canopy, where measurements are available from both the profile and eddy covariance systems. This suggests that, despite vertical stratification under stable atmospheric conditions, the dominant storage signal can be captured at a representative height, allowing the single-point approach to reliably reproduce long-term carbon exchange dynamics.

This result is particularly relevant because the time series of eddy covariance in Rebio Jaru is substantially longer than the period during which CO_2 profile measurements were available (See Fig. 2). Furthermore, $\mathrm{NEE_{SPP}}$ is considered more reliable than $\mathrm{NEE_{SPE}}$, because the latter was derived from measurements obtained with an open-path gas analyzer, which is generally more susceptible to environmental interferences such as rain, wind, and signal contamination than a closed-path system.

Conversely, the simplified approach of assuming $NEE = F_c$ yielded a substantially lower regression coefficient ($R^2 = 0.24$). This result demonstrates that neglecting the storage flux (F_s) is an inadequate approximation for dense forest sites, in

https://doi.org/10.5194/egusphere-2026-3167
Preprint. Discussion started: 19 June 2026

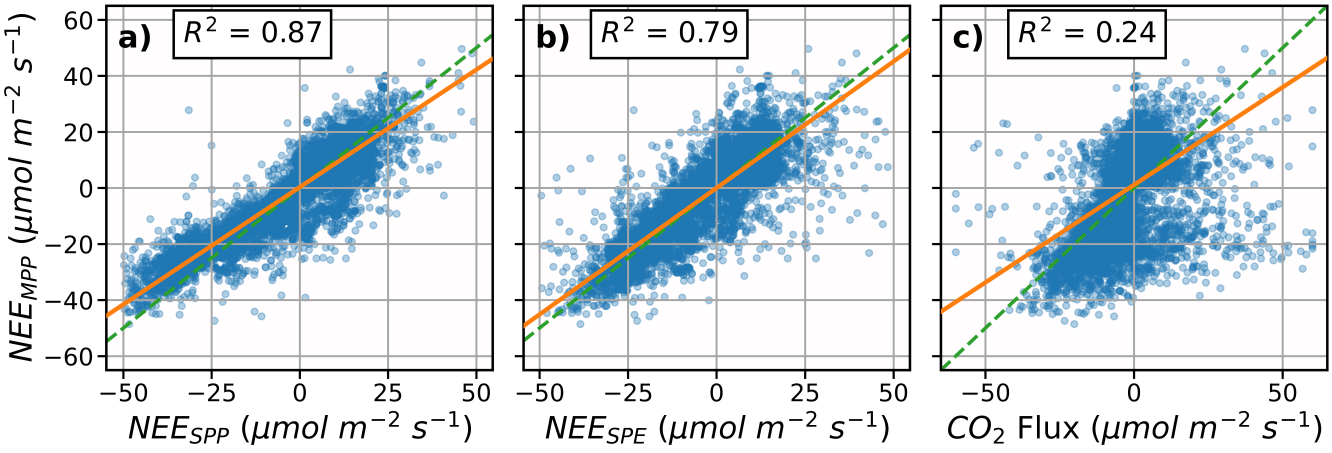

Figure 5. Relationship between the net ecosystem exchange (NEE) calculated using the storage flux (F_s) of the multi-point profile (NEE_{MPP}) and the NEE calculated using the following approaches for F_s: (a) single-point profile (NEE_{SPP}); (b) single-point eddy (NEE_{SPE}); and (c) $F_s = 0$, resulting in $NEE = F_c$. The analysis was performed using data from 2008 to 2009, when both the CO_2 profile and CO_2 flux measurements were available simultaneously. The solid line represents the linear regression fit, while the dashed line indicates the 1:1 relationship.

contrast to approaches adopted for savanna ecosystems in the Orinoco River region of the Colombian Amazon by Morales-Rincon et al. (2021). For Rebio Jaru, von Randow et al. (2004) and Cirino et al. (2014) occasionally relied on CO_2 flux measurements as a proxy for NEE when CO_2 profile observations were unavailable. Our results emphasize the critical importance of the storage estimates proposed here to minimize the underestimation of NEE in tall forests. Even when simplified proxies are applied, including a storage term provides a substantially more realistic representation of CO_2 dynamics than neglecting it entirely, while the MPP remains the most robust approach for representing ecosystem carbon exchange dynamics.

3.3 Interannual and Seasonal Variability of NEE

Since the SPE approach provided a reliable estimate of the storage term for the Rebio Jaru forest, we reconstructed the NEE time series for the entire period in which eddy covariance measurements were available. From this point onward, we assume $\mathrm{NEE} = \mathrm{NEE_{SPE}}$. Figure 6 presents the reconstructed time series from 1999 to 2020 as monthly accumulated values (Fig. 6b) and annual accumulated values (Fig. 6c), together with the Oceanic Niño Index (ONI; Fig. 6a).

The 1999–2000, 2000–2001, and 2007–2008 La Niña events coincided with periods during which Rebio Jaru generally acted as a carbon sink, as indicated by negative cumulative NEE values (Fig. 6b and Fig. 6c). However, despite the influence of the 2007–2008 La Niña event, the year 2008 exhibited a net carbon source behavior due to a pronounced emission peak during the late dry season, when La Niña conditions had already dissipated.

In contrast, following the 2002–2003 El Niño event, the forest frequently behaved as a carbon source and maintained this behavior during subsequent years, suggesting a possible drought legacy effect (Kannenberg et al., 2020; Wigneron et al., 2020;

https://doi.org/10.5194/egusphere-2026-3167
Preprint. Discussion started: 19 June 2026

Gonçalves et al., 2020). Previous studies have shown that severe droughts associated with El Niño events can produce persistent impacts on tropical forests, including enhanced tree mortality, delayed aboveground carbon recovery, and long-lasting alterations in leaf phenology and photosynthetic capacity. For example, Wigneron et al. (2020) demonstrated that tropical humid forests in the Americas did not fully recover their aboveground carbon stocks after the 2015–2016 El Niño drought, indicating prolonged ecosystem responses. Similarly, Gonçalves et al. (2020) reported persistent post-drought anomalies in canopy phenology and leaf demography in Amazon forests, suggesting that drought effects on ecosystem functioning may extend for more than one year after the climatic event.

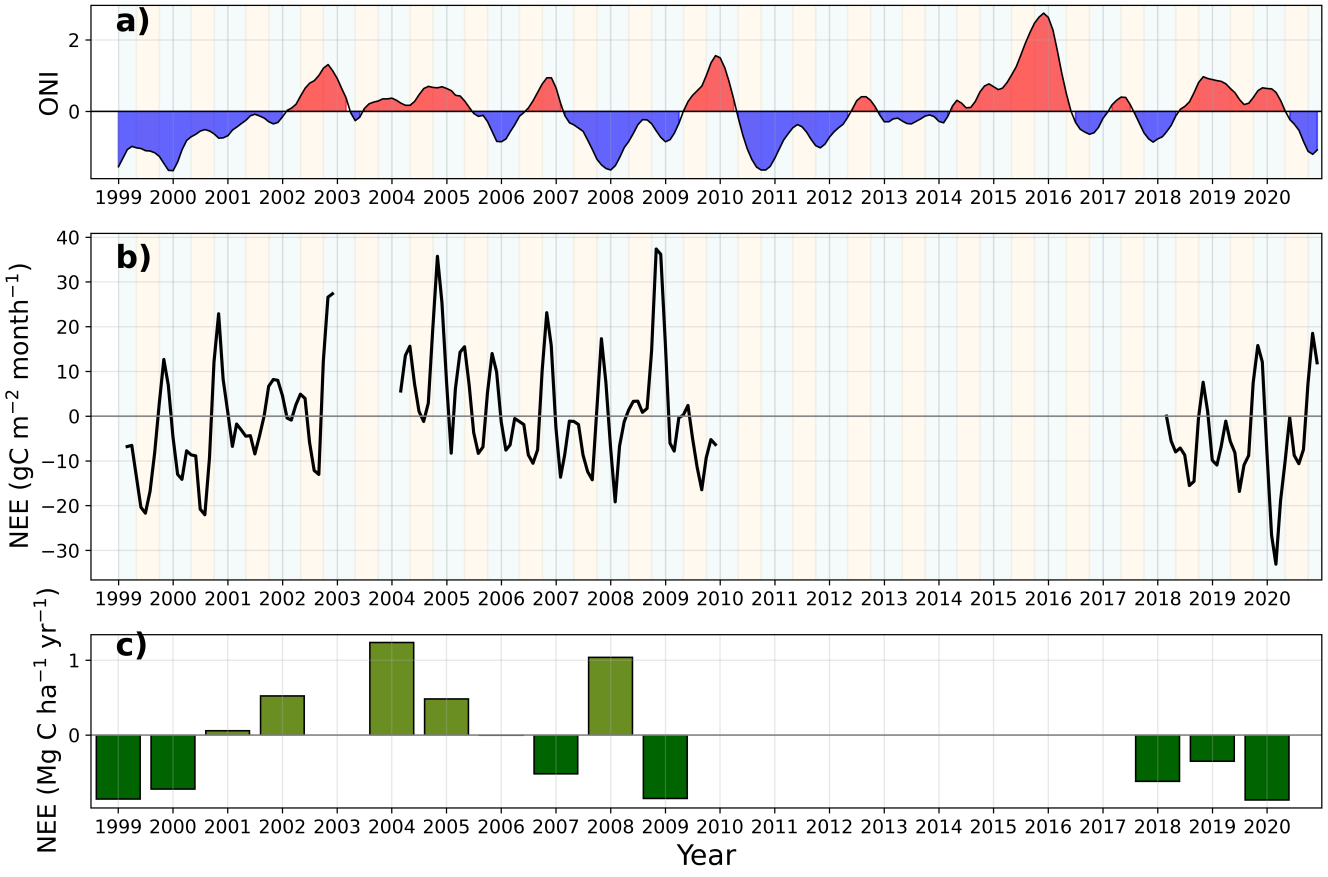

Figure 6. Time series of net ecosystem exchange (NEE) and the Oceanic Niño Index (ONI) at the Rebio Jaru site from 1999 to 2020. (a) Monthly ONI values, where positive anomalies (red) indicate El Niño conditions and negative anomalies (blue) indicate La Niña conditions. (b) Three-month running mean of monthly accumulated NEE expressed in g C m^{-2} month^{-1}. (c) Annual accumulated NEE expressed in Mg C ha^{-1} yr^{-1}. Negative NEE values indicate periods when the ecosystem acted as a carbon sink, while positive values indicate a carbon source. Years with insufficient or missing data (2003 and 2010–2017) were excluded from the analysis and represented as gaps in the time series.

https://doi.org/10.5194/egusphere-2026-3167
Preprint. Discussion started: 19 June 2026

Taken together, the results shown in Fig. 6 suggest that El Niño events weaken the ecosystem carbon sink, whereas La Niña events tend to enhance it. This pattern contrasts with the findings of Restrepo-Coupe et al. (2023) for central Amazonia, where enhanced carbon assimilation was observed during the 2015–2016 El Niño event, although the authors also reported evidence of drought legacy effects persisting after the event.

The seasonal cycle of NEE at Rebio Jaru (Fig. 7) exhibits a pronounced carbon source peak in October, coinciding with the transition between the late dry season and the onset of the wet season. This pattern differs from those reported by Hayek et al. (2018) and Restrepo-Coupe et al. (2023) for a tropical forest near Santarém, Pará, Brazil, as well as by Botía et al. (2022) at the Amazon Tall Tower Observatory (ATTO), near Manaus, Amazonas, Brazil.

A possible explanation for this peak is the semi-deciduous character of the Rebio Jaru forest, which likely experiences enhanced leaf senescence and litterfall during the dry season. The accumulated litter may then undergo rapid decomposition with the arrival of the first rains at the beginning of the wet season, increasing heterotrophic respiration and consequently enhancing CO_2 emissions from the soil to the atmosphere. This mechanism may contribute to the observed increase in ecosystem carbon release during this transition period.

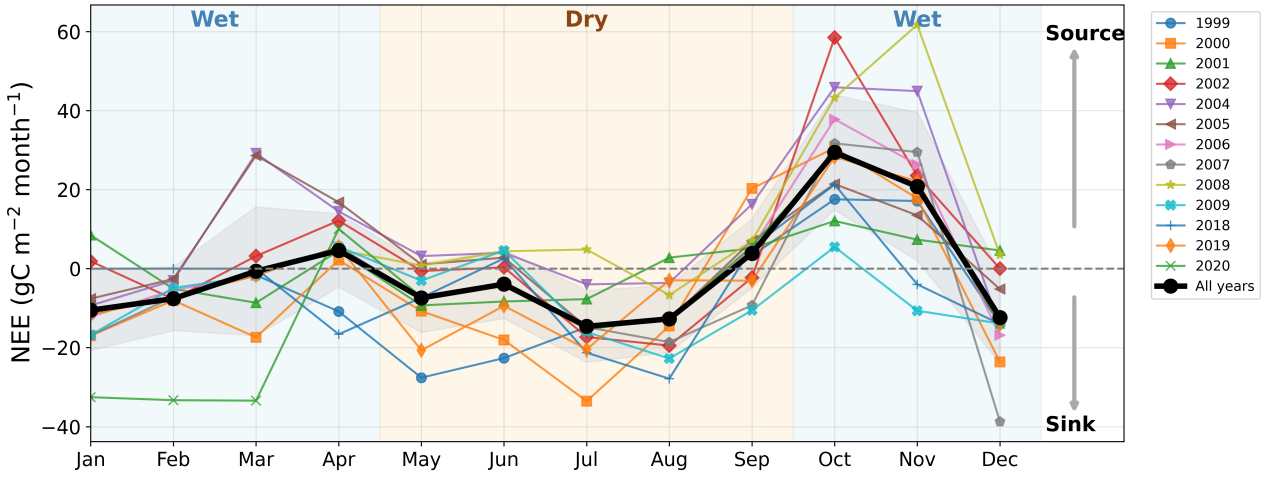

Figure 7. Seasonal cycle of monthly net ecosystem exchange (NEE) at Rebio Jaru for all available years. Colored lines represent individual years, while the thick black line indicates the climatological mean and the shaded gray region denotes ±1 standard deviation. Negative NEE values indicate net carbon uptake (sink), whereas positive values indicate net carbon release (source). Shaded background regions represent the wet season (October–April; blue) and dry season (May–September; orange).

For the same reason, a peak in CO_2 assimilation is observed in July, likely because ecosystem respiration is relatively low during this period while sufficient leaf area is still maintained to sustain high photosynthetic activity. During most of the remaining months, NEE remains close to carbon neutrality, except for pronounced source peaks observed in March 2004 and 2005, which may be associated with drought legacy effects following the 2002–2003 El Niño event. However, the mechanisms underlying these anomalies require further investigation and are beyond the scope of the present study. In contrast, the year

https://doi.org/10.5194/egusphere-2026-3167
Preprint. Discussion started: 19 June 2026

2020 exhibited a particularly strong carbon sink behavior, which also deserves a more detailed investigation to better understand the processes controlling this anomalous response.

4 Conclusions

This study demonstrates that reliable estimates of canopy CO_2 storage and net ecosystem exchange (NEE) can be obtained at Rebio Jaru using simplified single-height approaches when complete vertical CO_2 profile measurements are unavailable. The strong agreement between NEE derived from the traditional multi-point profile and the single-point profile approach ($R^2 = 0.87$), together with the good performance of the single-point eddy method ($R^2 = 0.79$), indicates that simplified storage estimates are capable of reproducing the dominant temporal variability of ecosystem carbon exchange in this tall Amazonian forest. In contrast, neglecting the storage term and assuming $NEE = F_c$ resulted in much poorer agreement ($R^2 = 0.24$), demonstrating that canopy CO_2 storage is an essential component of NEE at Rebio Jaru.

The comparison among atmospheric stability regimes showed that the performance of the simplified methods strongly depends on turbulence conditions. Both single-point approaches reproduced the multi-point profile more accurately under unstable and neutral conditions, whereas performance deteriorated under very stable nighttime conditions, especially for the single-point eddy method. Even so, the overall agreement between simplified and profile-based estimates supports the use of the single-point eddy approach to reconstruct long-term NEE variability at this site, particularly because the eddy covariance record is substantially longer than the available CO_2 profile measurements.

The reconstructed NEE time series revealed a strong influence of ENSO variability on the carbon balance of the Rebio Jaru forest. La Niña periods generally coincided with enhanced carbon uptake, whereas El Niño events were associated with weaker carbon sinks or even net carbon release. In particular, following the 2002–2003 El Niño event, the forest frequently behaved as a carbon source during subsequent years, suggesting the occurrence of drought legacy effects. These results indicate that interannual hydroclimatic variability exerts a stronger control on ecosystem carbon exchange than the regular seasonal cycle.

The seasonal cycle of NEE exhibited a pronounced carbon source peak during the transition from the dry to the wet season, particularly in October. This behavior differs from patterns reported for central and eastern Amazonian forests and may be associated with the semi-deciduous character of the Rebio Jaru forest. Enhanced litterfall during the dry season followed by rapid decomposition after the first rainfall events likely increases soil respiration and contributes to elevated CO_2 emissions during this transition period. Conversely, a peak in carbon uptake was observed during July, when ecosystem respiration is likely reduced while sufficient leaf area is maintained to sustain photosynthesis.

Overall, this study provides a practical framework for reconstructing long-term NEE at Amazonian flux towers where complete CO_2 profile measurements are intermittent or unavailable. These findings improve our understanding of carbon exchange dynamics in seasonally dry Amazon forests and highlight the importance of accurately representing canopy storage fluxes in studies of ecosystem carbon balance, atmospheric inversion modeling, and regional carbon budget assessments.

https://doi.org/10.5194/egusphere-2026-3167
Preprint. Discussion started: 19 June 2026

Code availability. The software code used in this study is publicly available in the Zenodo repository at 10.5281/zenodo.20534199 (Santana et al., 2026)

Data availability. The research data supporting this study are available through the Large-Scale Biosphere-Atmosphere Experiment in Amazonia (LBA) data request system at https://programa-lba.atlassian.net/servicedesk/customer/portal/1. Due to the consortium's data policy, access requires user registration and a formal data request through the platform.

Author contributions. B.A. conceived the study, processed the data, performed the analyses, and wrote the manuscript. R.A.S. contributed to data analysis, interpretation of the results, and manuscript revision. N.L.R.A., E.G.A., S.B., C.M.A.S., and S.K. contributed to field measurements, data processing, and scientific discussion. D.H.H., N.R.C., G.B.C., and C.Q.D.-J. contributed to the interpretation of the results and manuscript revision. C.Q.D.-J. supervised the study. All authors reviewed and approved the final manuscript.

Competing interests. The authors declare that they have no conflict of interest.

Acknowledgements. This research was supported as part of the Large-Scale Biosphere–Atmosphere Program in the Amazon (LBA), coordinated by the National Institute for Amazonian Research (INPA) and funded by the Brazilian Ministry of Science, Technology and Innovation (MCTI). The authors gratefully acknowledge the LBA program for supporting the long-term operation of the Rebio Jaru research site and the collection of the measurements used in this study. Cleo Q. Dias-Júnior gratefully acknowledges support from the Brazilian National Council for Scientific and Technological Development (CNPq) through grants 406884/2022-6, 307530/2022-1, 406307/2023-7, 444929/2024-0, 445451/2024-6, and 404254/2024-1.

https://doi.org/10.5194/egusphere-2026-3167
Preprint. Discussion started: 19 June 2026

References

Acevedo, O. C., Silva, R. D., Fitzjarrald, D. R., Moraes, O. L., Sakai, R. K., and Czikowsky, M. J.: Nocturnal vertical CO2 accumulation in two Amazonian ecosystems, Journal of Geophysical Research: Biogeosciences, 114, https://doi.org/10.1029/2007JG000612, 2009.

Aguiar, L. J. G., Fischer, G. R., Ladle, R. J., Malhado, A. C. M., Justino, F. B., Aguiar, R. G., and da Costa, J. M. N.: Modeling the photosynthetically active radiation in South West Amazonia under all sky conditions, Theoretical and Applied Climatology, 108, 631–640, https://doi.org/10.1007/s00704-011-0556-z, 2012.

Antonucci, B., Barbino, G. C., de Andrade, N. L. R., and Webler, A. D.: Efeito de um evento de friagem no cenário de mudança no uso e cobertura da terra no Sudoeste da Amazônia, Revista Brasileira de Climatologia, 33, 149–168, https://doi.org/10.55761/abclima.v33i19.16675, 2023.

Antonucci, B., Menezes, J. F. G., de Andrade, N. L. R., de Oliveira, G., Santos, C. A. G., Chaves, M. E. D., Mataveli, G., Schultze, S. R., and Webler, A. D.: Investigation of an unusual extreme precipitation event in the Jaru biological reserve, Brazilian Amazonia, Natural Hazards Research, 5, 898–906, https://doi.org/10.1016/j.nhres.2025.04.003, 2025.

Araújo, A., Nobre, A., Kruijt, B., Elbers, J., Dallarosa, R., Stefani, P., Randow, C. V., Manzi, A., Culf, A., Gash, J., Valentini, R., and Kabat, P.: Comparative measurements of carbon dioxide fluxes from two nearby towers in a central Amazonian rainforest: The Manaus LBA site, Journal of Geophysical Research, 107, 1–20, https://doi.org/10.1029/2001JD000676, 2002.

Araújo, A. C., Dolman, A. J., Waterloo, M. J., Gash, J. H., Kruijt, B., Zanchi, F. B., de Lange, J. M., Stoevelaar, R., Manzi, A. O., Nobre, A. D., Lootens, R. N., and Backer, J.: The Spatial Variability of CO_2 Storage and the Interpretation of Eddy Covariance Fluxes in Central Amazonia, Agricultural and Forest Meteorology, 150, 226–237, https://doi.org/10.1016/j.agrformet.2009.11.005, 2010.

Aubinet, M., Vesala, T., and Papale, D.: Eddy Covariance, Springer Netherlands, ISBN 978-94-007-2350-4, https://doi.org/10.1007/978-94-007-2351-1, 2012.

Baldocchi, D. and Meyers, P.: Turbulence structure in a deciduous forest, Boundary-Layer Meteorology, 43, 345–364, nULL, 1988.

Baldocchi, D., Novick, K., Keenan, T., and Torn, M.: AmeriFlux: Its Impact on our understanding of the 'breathing of the biosphere', after 25 years, Agricultural and Forest Meteorology, 348, 109 929, https://doi.org/10.1016/j.agrformet.2024.109929, 2024.

Barbino, G. C., de Andrade, N. L. R., Webler, A. D., Sanches, L., Aguiar, R., and Antonucci, B.: Índice de área foliar e sua relação com o microclima em floresta e pastagem na Amazônia Ocidental, Revista Brasileira de Climatologia, 32, 311–335, https://doi.org/10.55761/abclima.v32i19.16296, 2023.

Botía, S., Komiya, S., Marshall, J., Koch, T., Gałkowski, M., Lavric, J., Gomes-Alves, E., Walter, D., Fisch, G., Pinho, D. M., Nelson, B. W., Martins, G., Luijkx, I. T., Koren, G., Florentie, L., de Araújo, A. C., Sá, M., Andreae, M. O., Heimann, M., Peters, W., and Gerbig, C.: The CO2 record at the Amazon Tall Tower Observatory: A new opportunity to study processes on seasonal and inter-annual scales, Global Change Biology, 28, 588–611, https://doi.org/10.1111/gcb.15905, 2022.

Botía, S., Munassar, S., Koch, T., Custodio, D., Basso, L. S., Komiya, S., Lavric, J. V., Walter, D., Gloor, M., Martins, G., Naus, S., Koren, G., Luijkx, I. T., Hantson, S., Miller, J. B., Peters, W., Rödenbeck, C., and Gerbig, C.: Combined CO2 measurement record indicates Amazon forest carbon uptake is offset by savanna carbon release, Atmospheric Chemistry and Physics, 25, 6219–6255, https://doi.org/10.5194/acp-25-6219-2025, 2025.

Botía, S., Dias-Júnior, C. Q., Komiya, S., van der Woude, A. M., Terristi, M., de Kok, R. J., Koren, G., van Asperen, H., Jones, S. P., D'Oliveira, F. A. F., Weber, U., Marques-Filho, E. P., Cely, I. M., Araujo, A., Lavric, J. V., Walter, D., Li, X., Wigneron, J. P., Stocker, B. D., de Souza, J. G., O'Sullivan, M., Sitch, S., Ciais, P., Chevallier, F., Li, W., Luijkx, I., Peters, W., Quesada, C. A., Zaehle, S., Trumbore,

https://doi.org/10.5194/egusphere-2026-3167
Preprint. Discussion started: 19 June 2026

S., and Bastos, A.: Reduced Vegetation Uptake During the Extreme 2023 Drought Turns the Amazon Into a Weak Carbon Source, AGU Advances, 7, https://doi.org/10.1029/2025AV001658, 2026.

Buchmann, N., Guehl, J.-M., Barigah, T. S., and Ehleringer, J. R.: Interseasonal comparison of CO 2 concentrations, isotopic composition, and carbon dynamics in an Amazonian rainforest (French Guiana), Oecologia, 110, 120–131, https://doi.org/10.1007/s004420050140, 1997.

Chen, S., Stark, S. C., Nobre, A. D., Cuartas, L. A., de Jesus Amore, D., Restrepo-Coupe, N., Smith, M. N., Chitra-Tarak, R., Ko, H., Nelson, B. W., and Saleska, S. R.: Amazon forest biogeography predicts resilience and vulnerability to drought, Nature, 631, 111–117, https://doi.org/10.1038/s41586-024-07568-w, 2024.

Cirino, G. G., Souza, R. A. F., Adams, D. K., and Artaxo, P.: The effect of atmospheric aerosol particles and clouds on net ecosystem exchange in the Amazon, Atmospheric Chemistry and Physics, 14, 6523–6543, https://doi.org/10.5194/acp-14-6523-2014, 2014.

Costa, M. H., Biajoli, M. C., Sanches, L., Malhado, A. C., Hutyra, L. R., Rocha, H. R. D., Aguiar, R. G., and Araújo, A. C. D.: Atmospheric versus vegetation controls of Amazonian tropical rain forest evapotranspiration: Are the wet and seasonally dry rain forests any different?, Journal of Geophysical Research: Biogeosciences, 115, https://doi.org/10.1029/2009JG001179, 2010.

Csillik, O., Keller, M., Longo, M., Ferraz, A., Pinagé, E. R., Görgens, E. B., Ometto, J. P., Silgueiro, V., Brown, D., Duffy, P., Cushman, K. C., and Saatchi, S.: A large net carbon loss attributed to anthropogenic and natural disturbances in the Amazon Arc of Deforestation, Proceedings of the National Academy of Sciences of the United States of America, 121, https://doi.org/10.1073/pnas.2310157121, 2024.

Culf, A., Fisch, G., and Nobre, C.: AGRICULTURAL AND FOREST M ETEOROLOGY ELSEVIER The influence of the atmospheric boundary layer on carbgn dioxide concentrations over a tropical forest, Tech. rep., 1997.

Davidson, E. A., Araüjo, A. C. D., Artaxo, P., Balch, J. K., Brown, I. F., Mercedes, M. M., Coe, M. T., Defries, R. S., Keller, M., Longo, M., Munger, J. W., Schroeder, W., Soares-Filho, B. S., Souza, C. M., and Wofsy, S. C.: The Amazon basin in transition, https://doi.org/10.1038/nature10717, 2012.

de Oliveira, P. J., da Rocha, E. J. P., Fisch, G., Kruijt, B., and Ribeiro, J. B. M.: Efeitos de um evento de friagem nas condições meteorológicas na Amazônia: um estudo de caso, Acta Amazonica, 34, 613–619, https://doi.org/10.1590/S0044-59672004000400013, 2004.

Doughty, C. E., Metcalfe, D. B., Girardin, C. A., Amézquita, F. F., Cabrera, D. G., Huasco, W. H., Silva-Espejo, J. E., Araujo-Murakami, A., Costa, M. C. D., Rocha, W., Feldpausch, T. R., Mendoza, A. L., Costa, A. C. D., Meir, P., Phillips, O. L., and Malhi, Y.: Drought impact on forest carbon dynamics and fluxes in Amazonia, Nature, 519, 78–82, https://doi.org/10.1038/nature14213, 2015.

Feitosa, T. B., Fernandes, M. M., de Moura Fernandes, M. R., and Filho, R. N. A.: Temporal Analysis of Forest Fragmentation in the Amazon Rainforest of Tocantins State, Brazil, Floresta e Ambiente, 30, https://doi.org/10.1590/2179-8087-FLORAM-2022-0076, 2023.

Finnigan, J. J.: A Re-Evaluation of Long-Term Flux Measurement Techniques Part II: Coordinate Systems, Boundary-Layer Meteorology, 113, 1–41, https://doi.org/10.1023/B:BOUN.0000037348.64252.45, 2004.

Fisch, G., Tota, J., Machado, L. A. T., Dias, M. A. F. S., and Lyra, R. F. F.: The convective boundary layer over pasture and forest in Amazonia, Theor. Appl. Climatol., 59, 47–59, https://doi.org/10.1007/s00704-004-0043-x, 2004.

Flores, B. M., Montoya, E., Sakschewski, B., Nascimento, N., Staal, A., Betts, R. A., Levis, C., Lapola, D. M., Esquível-Muelbert, A., Jakovac, C., Nobre, C. A., Oliveira, R. S., Borma, L. S., Nian, D., Boers, N., Hecht, S. B., ter Steege, H., Arieira, J., Lucas, I. L., Berenguer, E., Marengo, J. A., Gatti, L. V., Mattos, C. R., and Hirota, M.: Critical transitions in the Amazon forest system, Nature, 626, 555–564, https://doi.org/10.1038/s41586-023-06970-0, 2024.

Garreaud, R.: Cold Air Incursions over Subtropical and Tropical South America: A Numerical Case Study, Monthly Weather Review, 127, 2823–2853, https://doi.org/10.1175/1520-0493(1999)127<2823:CAIOSA>2.0.CO;2, 1999.

https://doi.org/10.5194/egusphere-2026-3167
Preprint. Discussion started: 19 June 2026

Gatti, L. V., Basso, L. S., Miller, J. B., Gloor, M., Domingues, L. G., Cassol, H. L., Tejada, G., Aragão, L. E., Nobre, C., Peters, W., Marani, L., Arai, E., Sanches, A. H., Corrêa, S. M., Anderson, L., Randow, C. V., Correia, C. S., Crispim, S. P., and Neves, R. A.: Amazonia as a carbon source linked to deforestation and climate change, Nature, 595, 388–393, https://doi.org/10.1038/s41586-021-03629-6, 2021.

Gomes, J. B., Webler, A. D., Aguiar, R. G., Aguiar, L. J. G., and Nuñes, M. L. A.: Conversão de Florestas Tropicais em Sistemas Pecuários na Amazônia: Quais as Implicações no Microclima da Região?, Revista Brasileira de Climatologia, 17, https://doi.org/10.5380/abclima.v17i0.42879, 2015.

Gonçalves, N. B., Lopes, A. P., Dalagnol, R., Wu, J., Pinho, D. M., and Nelson, B. W.: Both near-surface and satellite remote sensing confirm drought legacy effect on tropical forest leaf phenology after 2015/2016 ENSO drought, Remote Sensing of Environment, 237, https://doi.org/10.1016/j.rse.2019.111489, 2020.

Google: Google Earth Pro, 2026.

Greco, S. and Baldocchi, D. D.: Seasonal variations of CO2 and water vapour exchange rates over a temperate deciduous forest, Global Change Biology, 2, 183–197, https://doi.org/10.1111/j.1365-2486.1996.tb00071.x, 1996.

Hayek, M. N., Longo, M., Wu, J., Smith, M. N., Restrepo-Coupe, N., Tapajós, R., Silva, R. D., Fitzjarrald, D. R., Camargo, P. B., Hutyra, L. R., Alves, L. F., Daube, B., Munger, J. W., Wiedemann, K. T., Saleska, S. R., and Wofsy, S. C.: Carbon exchange in an Amazon forest: From hours to years, Biogeosciences, 15, 4833–4848, https://doi.org/10.5194/bg-15-4833-2018, 2018.

Hollinger, D. Y., Kelliher, F. M., Byers, J. N., Hunt, J. E., McSeveny, T. M., and Weir, P. L.: Carbon dioxide exchange between an undisturbed old-growth temperate forest and the atmosphere, Ecology, 75, 134–150, https://doi.org/10.2307/1939390, 1994.

Hutyra, L. R., Munger, J. W., Hammond-Pyle, E., Saleska, S. R., Restrepo-Coupe, N., Daube, B. C., de Camargo, P. B., and Wofsy, S. C.: Resolving systematic errors in estimates of net ecosystem exchange of CO2 and ecosystem respiration in a tropical forest biome, Agricultural and Forest Meteorology, 148, 1266–1279, https://doi.org/10.1016/j.agrformet.2008.03.007, 2008.

IBGE: Base Cartográfica Contínua do Brasil ao Milionésimo (BCIM), 2022.

Kannenberg, S. A., Schwalm, C. R., and Anderegg, W. R.: Ghosts of the past: how drought legacy effects shape forest functioning and carbon cycling, https://doi.org/10.1111/ele.13485, 2020.

Marengo, J. A., Espinoza, J. C., Fu, R., Muñoz, J. C. J., Alves, L. M., Rocha, H. R. D., and Schöngart, J.: Long-term variability, extremes and changes in temperature and hydrometeorology in the Amazon region: A review, Acta Amazonica, 54, https://doi.org/10.1590/1809-4392202200980, 2024.

Miller, S. D., Goulden, M. L., Menton, M. C., Rocha, H. R. D., Freitas, H. C. D., Figueira, A. M. E. S., and Sousa, C. A. D. D.: Biometric and micrometeorological measurements of tropical forest carbon balance, Ecological Applications, 14, https://doi.org/10.1890/02-6005, 2004.

Moureaux, C., Debacq, A., Hoyaux, J., Suleal, M., Tourneur, D., Vancutsem, F., Bodson, B., and Marc, A.: Carbon balance assessment of a Belgian winter wheat crop (Triticum aestivum L.), Global Change Biology, 14, 1353–1366, https://doi.org/10.1111/j.1365-2486.2008.01560.x, 2008.

Pastorello, G., Trotta, C., Canfora, E., Chu, H., Christianson, D., Cheah, Y. W., Poindexter, C., Chen, J., Elbashandy, A., Humphrey, M., Isaac, P., Polidori, D., Ribeca, A., van Ingen, C., Zhang, L., Amiro, B., Ammann, C., Arain, M. A., Ardö, J., Arkebauer, T., Arndt, S. K., Arriga, N., Aubinet, M., Aurela, M., Baldocchi, D., Barr, A., Beamesderfer, E., Marchesini, L. B., Bergeron, O., Beringer, J., Bernhofer, C., Berveiller, D., Billesbach, D., Black, T. A., Blanken, P. D., Bohrer, G., Boike, J., Bolstad, P. V., Bonal, D., Bonnefond, J. M., Bowling, D. R., Bracho, R., Brodeur, J., Brümmer, C., Buchmann, N., Burban, B., Burns, S. P., Buysse, P., Cale, P., Cavagna, M., Cellier, P., Chen, S., Chini, I., Christensen, T. R., Cleverly, J., Collalti, A., Consalvo, C., Cook, B. D., Cook, D., Coursolle, C., Cremonese, E., Curtis, P. S.,

https://doi.org/10.5194/egusphere-2026-3167
Preprint. Discussion started: 19 June 2026

D'Andrea, E., da Rocha, H., Dai, X., Davis, K. J., Cinti, B. D., de Grandcourt, A., Ligne, A. D., Oliveira, R. C. D., Delpierre, N., Desai, A. R., Bella, C. M. D., di Tommasi, P., Dolman, H., Domingo, F., Dong, G., Dore, S., Duce, P., Dufrêne, E., Dunn, A., Dušek, J., Eamus, D., Eichelmann, U., ElKhidir, H. A. M., Eugster, W., Ewenz, C. M., Ewers, B., Famulari, D., Fares, S., Feigenwinter, I., Feitz, A., Fensholt, R., Filippa, G., Fischer, M., Frank, J., Galvagno, M., Gharun, M., Gianelle, D., Gielen, B., Gioli, B., Gitelson, A., Goded, I., Goeckede, M., Goldstein, A. H., Gough, C. M., Goulden, M. L., Graf, A., Griebel, A., Gruening, C., Grünwald, T., Hammerle, A., Han, S., Han, X., Hansen, B. U., Hanson, C., Hatakka, J., He, Y., Hehn, M., Heinesch, B., Hinko-Najera, N., Hörtnagl, L., Hutley, L., Ibrom, A., Ikawa, H., Jackowicz-Korczynski, M., Janouš, D., Jans, W., Jassal, R., Jiang, S., Kato, T., Khomik, M., Klatt, J., Knohl, A., Knox, S., Kobayashi, H., Koerber, G., Kolle, O., Kosugi, Y., Kotani, A., Kowalski, A., Kruijt, B., Kurbatova, J., Kutsch, W. L., Kwon, H., Launiainen, S., Laurila, T., Law, B., Leuning, R., Li, Y., Liddell, M., Limousin, J. M., Lion, M., Liska, A. J., Lohila, A., López-Ballesteros, A., López-Blanco, E., Loubet, B., Loustau, D., Lucas-Moffat, A., Lüers, J., Ma, S., Macfarlane, C., Magliulo, V., Maier, R., Mammarella, I., Manca, G., Marcolla, B., Margolis, H. A., Marras, S., Massman, W., Mastepanov, M., Matamala, R., Matthes, J. H., Mazzenga, F., McCaughey, H., McHugh, I., McMillan, A. M., Merbold, L., Meyer, W., Meyers, T., Miller, S. D., Minerbi, S., Moderow, U., Monson, R. K., Montagnani, L., Moore, C. E., Moors, E., Moreaux, V., Moureaux, C., Munger, J. W., Nakai, T., Neirynck, J., Nesic, Z., Nicolini, G., Noormets, A., Northwood, M., Nosetto, M., Nouvellon, Y., Novick, K., Oechel, W., Olesen, J. E., Ourcival, J. M., Papuga, S. A., Parmentier, F. J., Paul-Limoges, E., Pavelka, M., Peichl, M., Pendall, E., Phillips, R. P., Pilegaard, K., Pirk, N., Posse, G., Powell, T., Prasse, H., Prober, S. M., Rambal, S., Üllar Rannik, Raz-Yaseef, N., Reed, D., de Dios, V. R., Restrepo-Coupe, N., Reverter, B. R., Roland, M., Sabbatini, S., Sachs, T., Saleska, S. R., Sánchez-Cañete, E. P., Sanchez-Mejia, Z. M., Schmid, H. P., Schmidt, M., Schneider, K., Schrader, F., Schroder, I., Scott, R. L., Sedlák, P., Serrano-Ortíz, P., Shao, C., Shi, P., Shironya, I., Siebicke, L., Šigut, L., Silberstein, R., Sirca, C., Spano, D., Steinbrecher, R., Stevens, R. M., Sturtevant, C., Suyker, A., Tagesson, T., Takanashi, S., Tang, Y., Tapper, N., Thom, J., Tiedemann, F., Tomassucci, M., Tuovinen, J. P., Urbanski, S., Valentini, R., van der Molen, M., van Gorsel, E., van Huissteden, K., Varlagin, A., Verfaillie, J., Vesala, T., Vincke, C., Vitale, D., Vygodskaya, N., Walker, J. P., Walter-Shea, E., Wang, H., Weber, R., Westermann, S., Wille, C., Wofsy, S., Wohlfahrt, G., Wolf, S., Woodgate, W., Li, Y., Zampedri, R., Zhang, J., Zhou, G., Zona, D., Agarwal, D., Biraud, S., Torn, M., and Papale, D.: The FLUXNET2015 dataset and the ONEFlux processing pipeline for eddy covariance data, Scientific Data, 7, https://doi.org/10.1038/s41597-020-0534-3, 2020.

Paul-Limoges, E., Wolf, S., Eugster, W., Hörtnagl, L., and Buchmann, N.: Below-canopy contributions to ecosystem CO_2 fluxes in a temperate mixed forest in Switzerland, Agricultural and Forest Meteorology, 247, 582–596, https://doi.org/10.1016/j.agrformet.2017.08.011, 2017.

Peltola, O., Lapo, K., Martinkauppi, I., O'Connor, E., Thomas, C. K., and Vesala, T.: Suitability of fibre-optic distributed temperature sensing for revealing mixing processes and higher-order moments at the forest-air interface, Atmospheric Measurement Techniques, 14, 2409–2427, https://doi.org/10.5194/amt-14-2409-2021, 2021.

Reichstein, M., Falge, E., Baldocchi, D., Papale, D., Aubinet, M., Berbigier, P., Bernhofer, C., Buchmann, N., Gilmanov, T., Granier, A., Grünwald, T., Havránková, K., Ilvesniemi, H., Janous, D., Knohl, A., Laurila, T., Lohila, A., Loustau, D., Matteucci, G., Meyers, T., Miglietta, F., Ourcival, J. M., Pumpanen, J., Rambal, S., Rotenberg, E., Sanz, M., Tenhunen, J., Seufert, G., Vaccari, F., Vesala, T., Yakir, D., and Valentini, R.: On the separation of net ecosystem exchange into assimilation and ecosystem respiration: Review and improved algorithm, https://doi.org/10.1111/j.1365-2486.2005.001002.x, 2005.

Restrepo-Coupe, N., O'Donnell Christoffersen, B., Longo, M., Alves, L. F., Campos, K. S., da Araujo, A. C., de Oliveira, R. C., Prohaska, N., da Silva, R., Tapajos, R., Wiedemann, K. T., Wofsy, S. C., and Saleska, S. R.: Asymmetric response of Amazon forest water and

https://doi.org/10.5194/egusphere-2026-3167
Preprint. Discussion started: 19 June 2026

energy fluxes to wet and dry hydrological extremes reveals onset of a local drought-induced tipping point, Global Change Biology, 29, 6077–6092, https://doi.org/10.1111/gcb.16933, 2023.

Rodrigues, J. R., Solander, K. C., Cropper, S., Newman, B. D., Collins, A. D., Warren, J. M., Negron-Juarez, R., Gimenez, B. O., Spanner, G. C., da Silva Menezes, V., Ríos-Villamizar, E. A., de Oliveira, R. C., Ferreira, S. J. F., and Higuchi, N.: Soil water percolation and nutrient fluxes as a function of topographical, seasonal and soil texture variation in Central Amazonia, Brazil, Hydrological Processes, 38, https://doi.org/10.1002/hyp.15148, 2024.

Rummel, U., Ammann, C., Gut, A., Meixner, F. X., and Andreae, M. O.: Eddy covariance measurements of nitric oxide flux within ah Amazonian rain forest, Journal of Geophysical Research: Atmospheres, 107, LBA 17–1–LBA 17–9, https://doi.org/10.1029/2001JD000520, 2002.

Saito, M., Miyata, A., Nagai, H., and Yamada, T.: Seasonal variation of carbon dioxide exchange in rice paddy field in Japan, Agricultural and Forest Meteorology, 135, 93–109, https://doi.org/10.1016/j.agrformet.2005.10.007, 2005.

Santana, R., Dias-Júnior, C., Tóta, J., Fuentes, J., Vale, R., Alves, E., Santos, R., and Manzi, A.: Air turbulence characteristics at multiple sites in and above the Amazon rainforest canopy, Agricultural and Forest Meteorology, 260-261, 41–54, https://doi.org/10.1016/j.agrformet.2018.05.027, 2018.

Santana, R. A. S., Antonucci, B., and Dias-Júnior, C. Q.: Amazon Carbon Flux Analysis, https://doi.org/https://doi.org/10.5281/zenodo.20693456, 2026.

Tavares, J. V., Oliveira, R. S., Mencuccini, M., Signori-Müller, C., Pereira, L., Diniz, F. C., Gilpin, M., Zevallos, M. J. M., Yupayccana, C. A. S., Acosta, M., Mullisaca, F. M. P., de V. Barros, F., Bittencourt, P., Jancoski, H., Scalon, M. C., Marimon, B. S., Menor, I. O., Marimon, B. H., Fancourt, M., Chambers-Ostler, A., Esquivel-Muelbert, A., Rowland, L., Meir, P., da Costa, A. C. L., Nina, A., Sanchez, J. M., Tintaya, J. S., Chino, R. S., Baca, J., Fernandes, L., Cumapa, E. R., Santos, J. A. R., Teixeira, R., Tello, L., Ugarteche, M. T., Cuellar, G. A., Martinez, F., Araujo-Murakami, A., Almeida, E., da Cruz, W. J. A., del Aguila Pasquel, J., Aragão, L., Baker, T. R., de Camargo, P. B., Brienen, R., Castro, W., Ribeiro, S. C., de Souza, F. C., Cosio, E. G., Cardozo, N. D., da Costa Silva, R., Disney, M., Espejo, J. S., Feldpausch, T. R., Ferreira, L., Giacomin, L., Higuchi, N., Hirota, M., Honorio, E., Huasco, W. H., Lewis, S., Llampazo, G. F., Malhi, Y., Mendoza, A. M., Morandi, P., Moscoso, V. C., Muscarella, R., Penha, D., Rocha, M. C., Rodrigues, G., Ruschel, A. R., Salinas, N., Schlickmann, M., Silveira, M., Talbot, J., Vásquez, R., Vedovato, L., Vieira, S. A., Phillips, O. L., Gloor, E., and Galbraith, D. R.: Basin-wide variation in tree hydraulic safety margins predicts the carbon balance of Amazon forests, Nature, 617, 111–117, https://doi.org/10.1038/s41586-023-05971-3, 2023.

Trejo, P., Azevedo-Ramos, C., and Lenti, F.: Forest fragmentation in the Brazilian Amazon: Trends and conservation strategies, Perspectives in Ecology and Conservation, 23, 104–109, https://doi.org/10.1016/j.pecon.2025.04.001, 2025.

Tóta, J., Fitzjarrald, D. R., Staebler, R. M., Sakai, R. K., Moraes, O. M. M., Acevedo, O. C., Wofsy, S. C., and Manzi, A. O.: Amazon rain forest subcanopy flow and the carbon budget: Santarém LBA-ECO site, Journal of Geophysical Research: Biogeosciences, 114, 1–15, https://doi.org/10.1029/2007JG000597, 2008.

von Randow, C., Manzi, A. O., Kruijt, B., de Oliveira, P. J., Zanchi, F. B., Silva, R. L., Hodnett, M. G., Gash, J. H. C., Elbers, J. A., Waterloo, M. J., Cardoso, F. L., and Kabat, P.: Comparative measurements and seasonal variations in energy and carbon exchange over forest and pasture in South West Amazonia, Theoretical and Applied Climatology, 78, 5–26, https://doi.org/10.1007/s00704-004-0041-z, 2004.

Wigneron, J.-P., Fan, L., Ciais, P., Bastos, A., Brandt, M., Chave, J., Saatchi, S., Baccini, A., and Fensholt, R.: Tropical Forests Did Not Recover from the Strong 2015–2016 El Niño Event, Tech. rep., https://www.science.org, 2020.